The h Channel Mediates Location Dependence and Plasticity of Intrinsic Phase Response in Rat Hippocampal Neurons

Rishikesh Narayanan and Daniel Johnston

Center for Learning and Memory,
The University of Texas at Austin, Austin, TX 78712

The Journal of Neuroscience, 28 May 2008, 28(22): 5846–5860

SUPPLEMENTAL MATERIAL

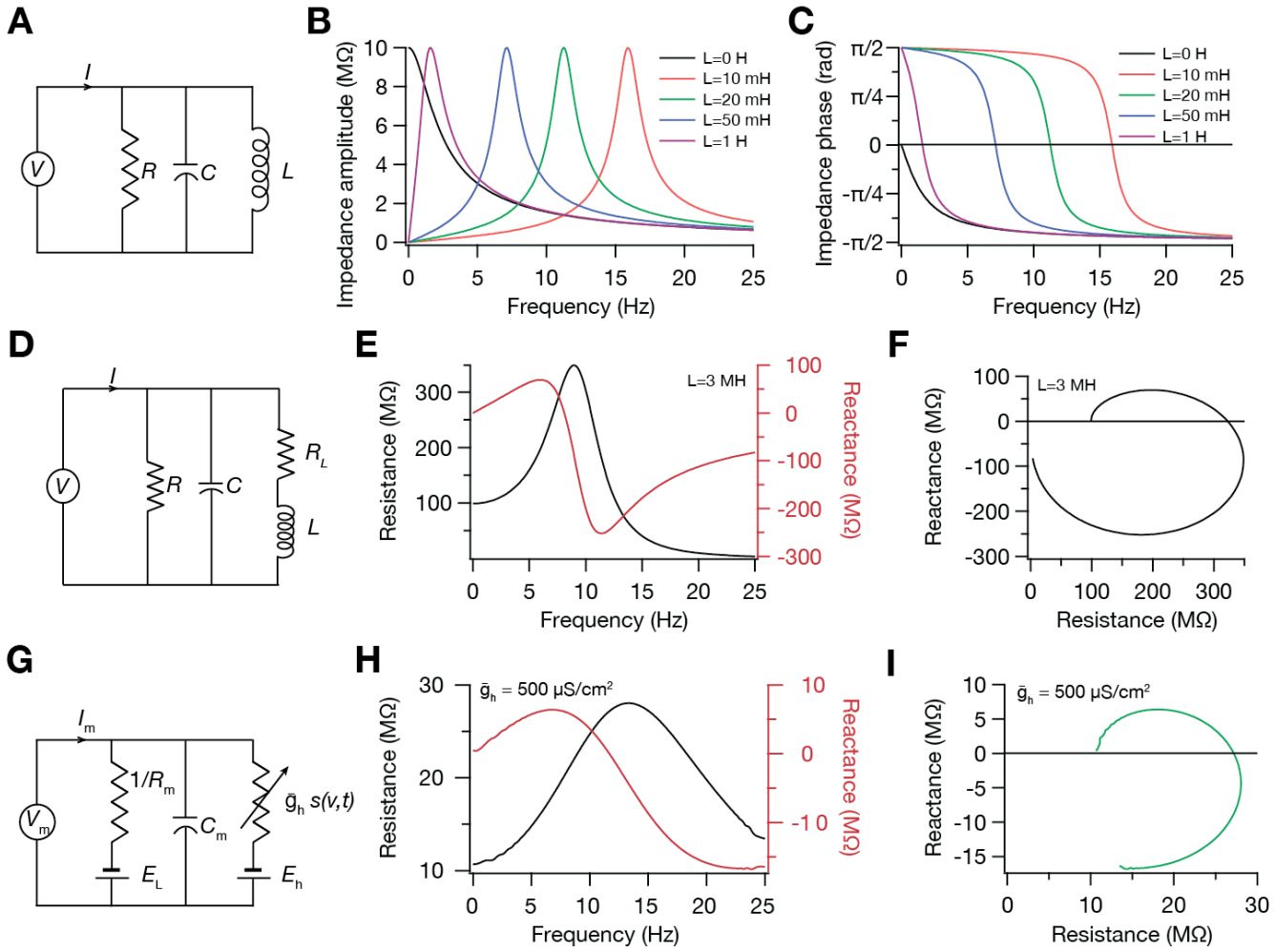

Supplemental Figure 1. ***A***, *RCL* circuit with an ideal inductor. The values of parameters used for plots in ***B***–***C*** were R=10 Ω and C=10 mF. ***B***, Impedance amplitude profiles for various values of L. For nonzero values of L, the circuit acts as a band pass filter, and its resonance frequency increases with reduction in L. ***C***, Impedance phase profile for various values of L. It may be noted that the impedance phase is positive up to a certain crossover frequency after which it turns negative. For non-zero values of L, the crossover frequency increases with reduction in L. Plots in ***B***–***C*** were obtained from analytical expressions for impedance amplitude and phase of the circuit in ***A***. ***D***, *RCL* circuit with a leaky inductor. The parameters are the same as Fig. 1. Resistance and reactance plotted as functions of frequency (***E***) and the reactance-resistance locus plot (***F***) for the circuit in ***D*** are shown. Plots in ***E***–***F*** were obtained from analytical expressions for impedance amplitude and phase of the circuit in *D*. ***G***, *RCh* circuit representing a single compartment neuron model, with the *h* conductance as the only active mechanism. Resistance and reactance plotted as functions of frequency (***H***) and the reactance-resistance locus plot (***I***) for the circuit in ***G*** are shown. Note that the resistance, reactance and reactance-resistance plots for the circuits in ***D*** and ***G*** are similar to each other.

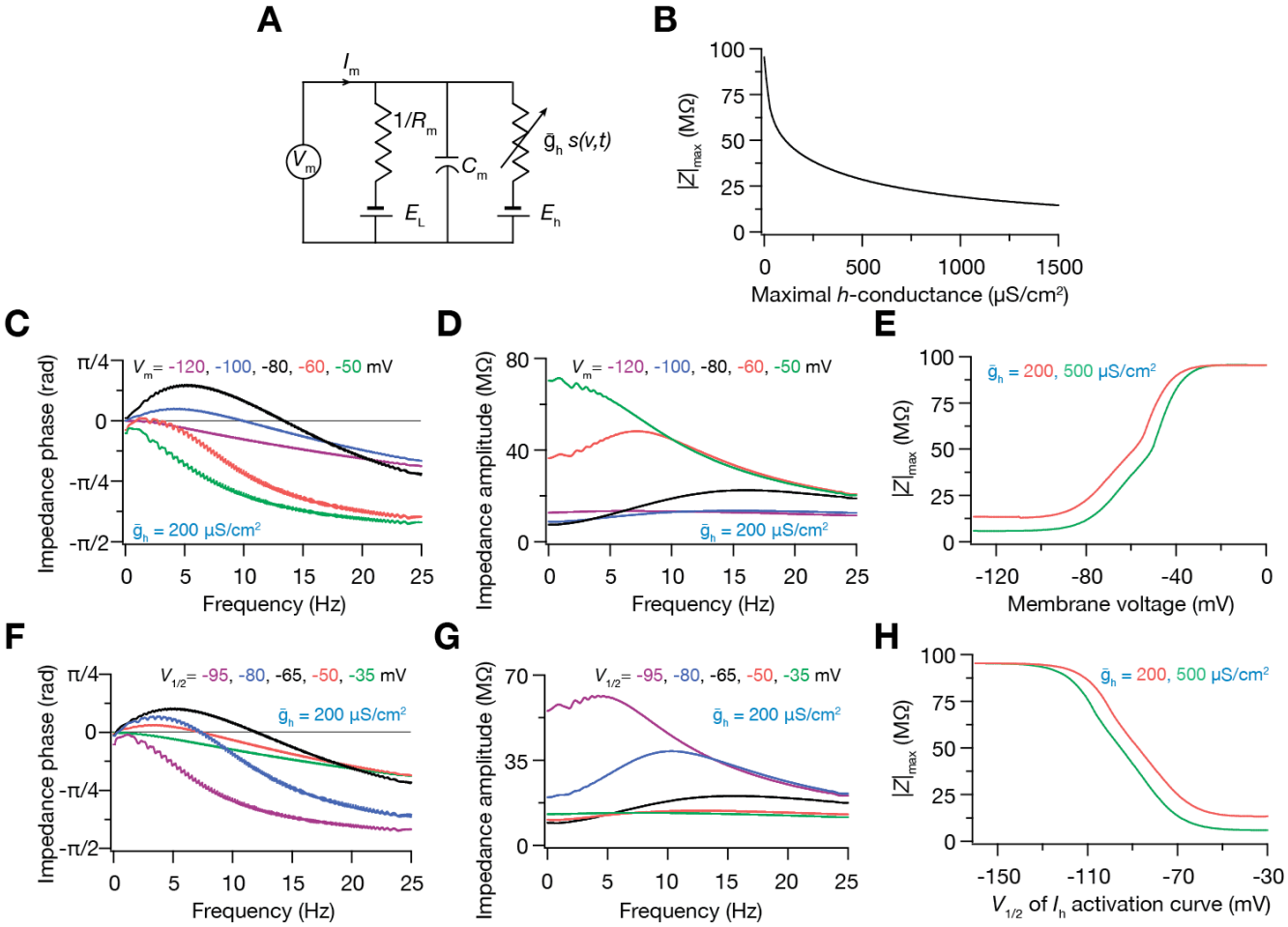

Supplemental Figure 2. ***A***, *RCh* circuit representing a single compartment neuron model, with the *h* conductance as the only active mechanism. ***B***, Plot depicting the decrease in maximal impedance amplitude $|Z|_{max}$ as a function of maximal *h* conductance. Impedance phase (***C***) and amplitude (***D***) profiles for various values of membrane voltage are shown. ***E***, Plot showing the increase in $|Z|_{max}$ with membrane depolarization. Impedance phase (***F***) and amplitude (***G***) profiles for various values of the half-maximal activation voltage of the *h* conductance. ***H***, Plot showing the reduction in $|Z|_{max}$ with the half-maximal activation voltage of the *h* conductance.

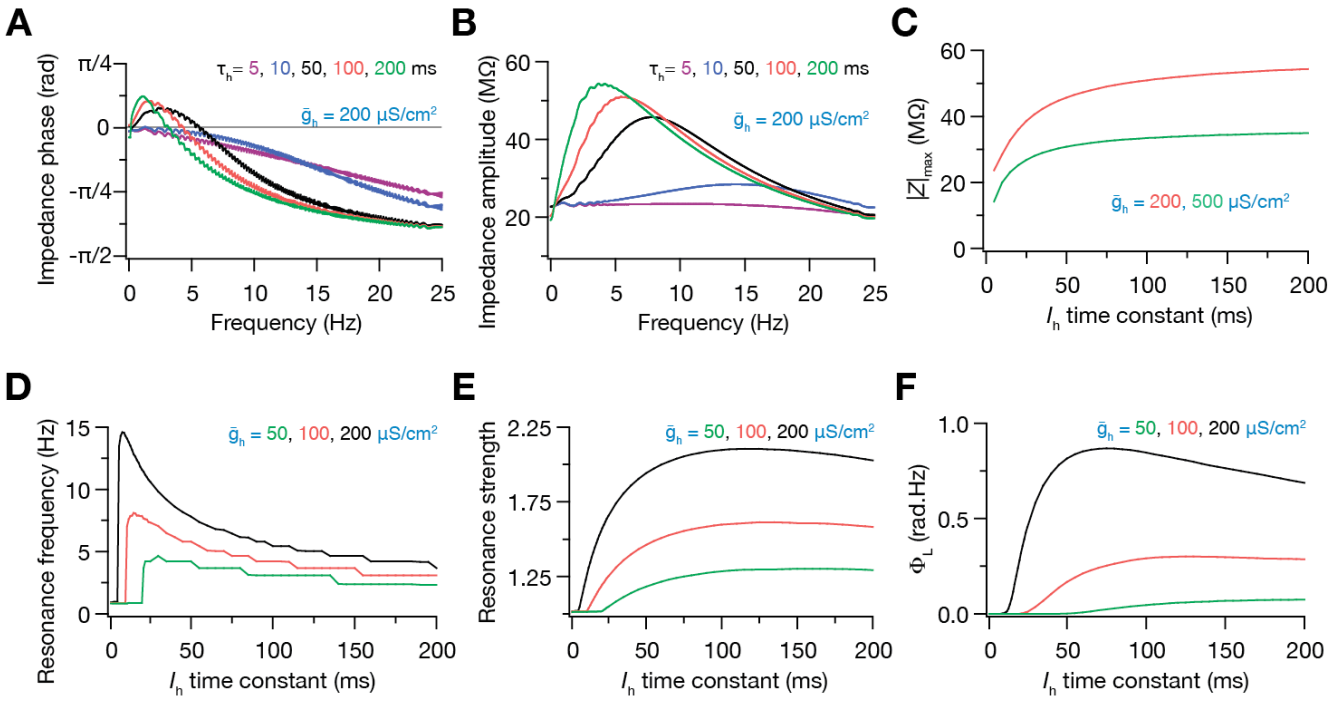

Supplemental Figure 3. These plots continue with parametric dependence of various impedance measurements from the *RCh* circuit from Supplementary Fig. 2. Impedance phase (***A***) and amplitude (***B***) profiles for various values of the activation/deactivation time constant of the *h* conductance (τ_h) are shown. The striking similarity between the impedance plots in Fig. 1 for increasing *L* and those in ***A***–***B*** for increasing τ_h may be noted, suggesting that τ_h contributes exclusively to the inductive part of the leaky inductor that the *h* conductance contributes (Fig. 1 & 2). The increase in maximal impedance amplitude $|Z|_{max}$ (***C***) and reduction in resonance frequency (***D***) with increasing τ_h are plotted. It may be noted from ***D*** that resonance does not express if τ_h is lesser than a certain value, and that this threshold reduces with increase in the maximal *h* conductance, $\bar{g}_h$. Once this threshold is crossed, resonance frequency decreases with increase in τ_h, although the rate of reduction is dependent on the value of $\bar{g}_h$ (***D***). Dependencies of resonance strength and total inductive phase, Φ_L, on τ_h are shown in ***E*** and ***F*** respectively. It may be also noted that this threshold value on τ_h reduces with increase in $\bar{g}_h$ (***D***–***F***).

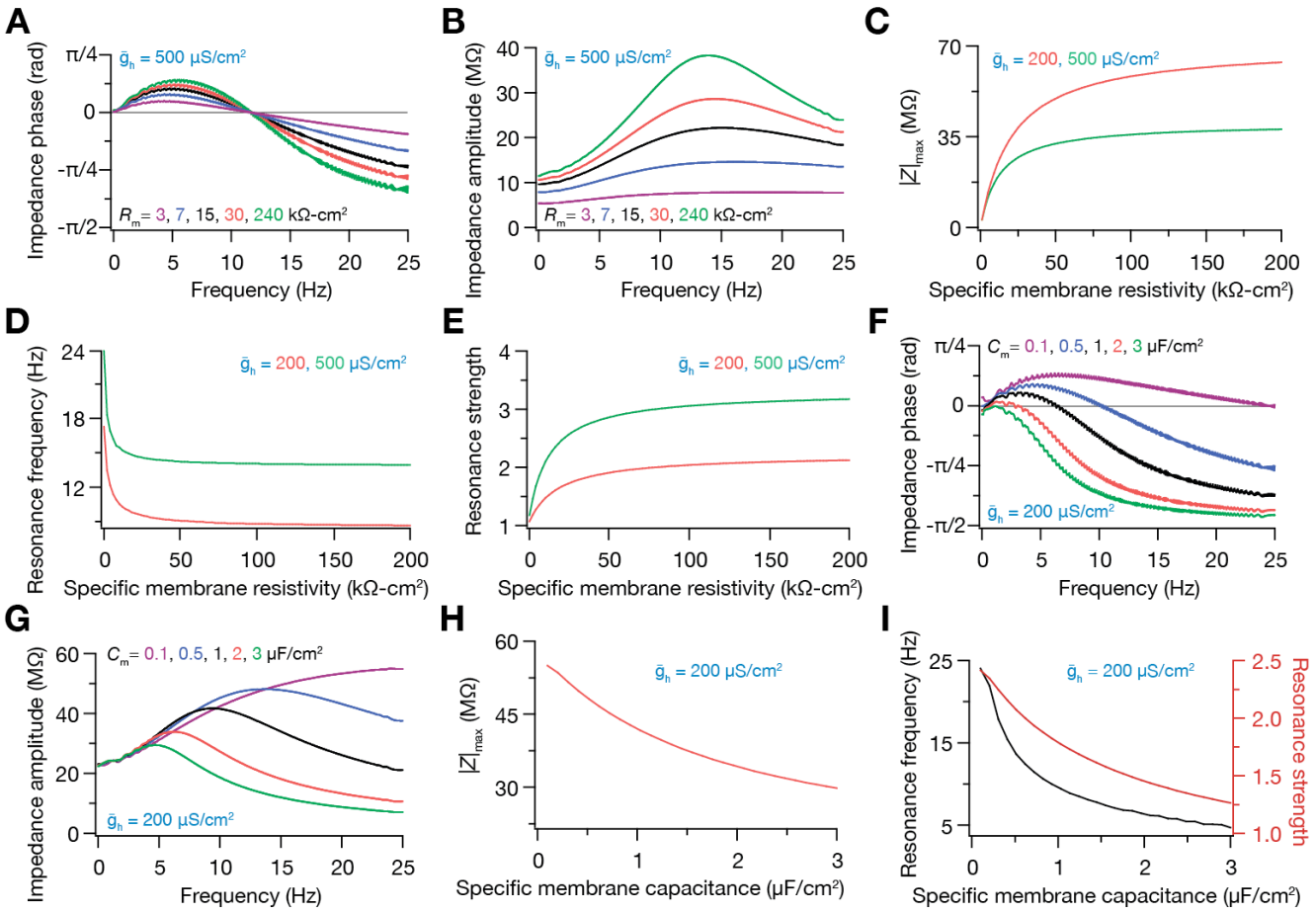

Supplemental Figure 4. These plots continue with parametric dependence of various impedance measurements from the *RCh* circuit from Supplementary Figs. 2–3. Impedance phase (***A***) and amplitude (***B***) profiles for various values of specific membrane resistivity (R_m) are shown. The increase in maximal impedance amplitude $|Z|_{max}$ (***C***), reduction in resonance frequency (***D***), and increase in resonance strength (***E***) with increasing R_m are noted. Impedance phase (***F***) and amplitude (***G***) profiles for various values of specific membrane capcitance (C_m) are shown. The decrease in maximal impedance amplitude $|Z|_{max}$ (***H***), reduction in resonance frequency and resonance strength (***I***) with increasing C_m are also noted.

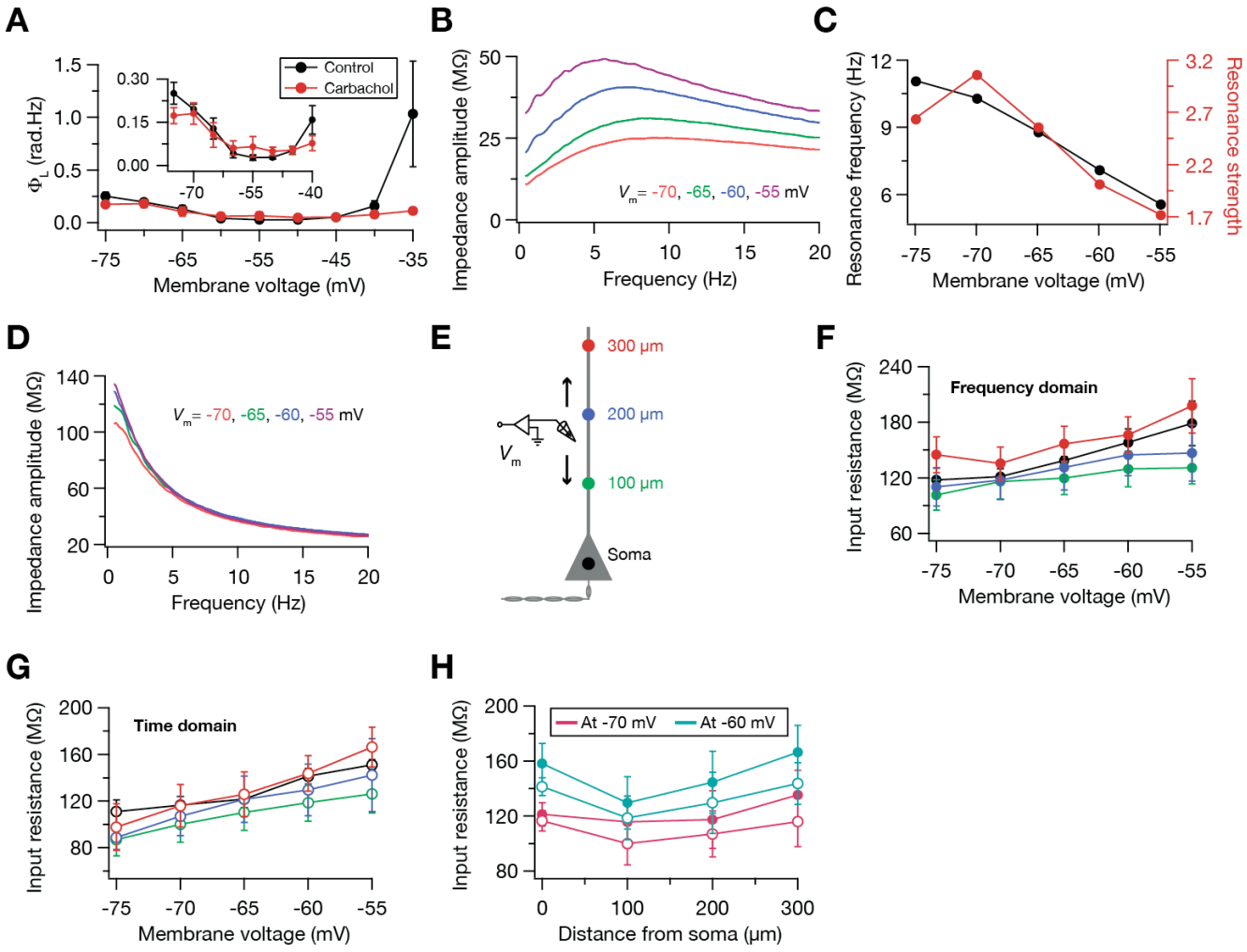

Supplemental Figure 5. ***A,*** The *M*-type potassium channel contributes an inductive component to the input impedance of CA1 pyramidal neurons at more depolarized voltages. Whole-cell patch-clamp recordings from CA1 pyramidal neuron soma were performed in the presence of 10 µM CNQX, 10 µM (+)bicuculline, 10 µM picrotoxin, 50 µM D, L-APV, 2 µM CGP55845, 1 µM TTX and 2 mM $NiCl_2$. The increase total inductive phase, Φ_L, in the hyperpolarized voltage range (–75 mV to –55 mV; Control) is consistent with data presented in (Fig. 4), and is mediated by the *h*-channel (Fig. 5). Increase in Φ_L at more depolarized voltages (–50 mV to –35 mV; Control) is dependent on the *M*-type potassium current, as 10 µM Carbachol, a muscarinic agonist, in the bath abolishes resonance in that voltage range, without affecting Φ_L in hyperpolarized voltages (Carbachol). Inset shows the same plot in the –75 mV to –40 mV just to emphasize the lack of changes in Φ_L in the presence of Carbachol. Control *N*=6; Carbachol *N*=5. ***B***, Experimentally obtained impedance amplitude profiles at various membrane voltages for the dendritic recordings shown in Fig. 4*A*. ***C***, Resonance frequency and resonance strength computed from the impedance amplitude profiles shown in ***B*** indicate the increase in both these parameters with hyperpolarization. ***D****,* Experimentally obtained impedance amplitude profiles at various membrane voltages for the dendritic recordings shown in Fig. 5*A*. The resonance frequency was less than unity, and the resonance strength was close to unity for all these profiles. ***E***, Schematic of the somato-apical trunk, depicting the experimental design for estimating input resistance as a function of

distance from the soma. In ZD7288 pretreated slices, voltage responses of the soma and dendrites at various distances (up to 300 μm away from the soma) to the *Chirp20* stimulus and to a hyperpolarizing current pulse (100 pA) were recorded locally using a whole-cell patch-clamp electrode (V_m). The response to the *Chirp20* stimulus and the hyperpolarizing pulse were used to estimate input resistance in the frequency domain (***F***) and in the time domain (***G***) respectively. Colors of markers serve as codes for corresponding distances in ***F***–***G***. The plots of local input resistance estimated using frequency (***F***) and time (***G***) domain methods as a function of membrane voltage for various distances, and as functions of distance from the soma (***H***) are provided. In ***H***, closed and open circles indicate frequency and time domain estimates, respectively. These plots show that local input resistance does not significantly change with distance from the soma, and that the estimates obtained from time and frequency domain methods were not significantly different across various distances from the soma.

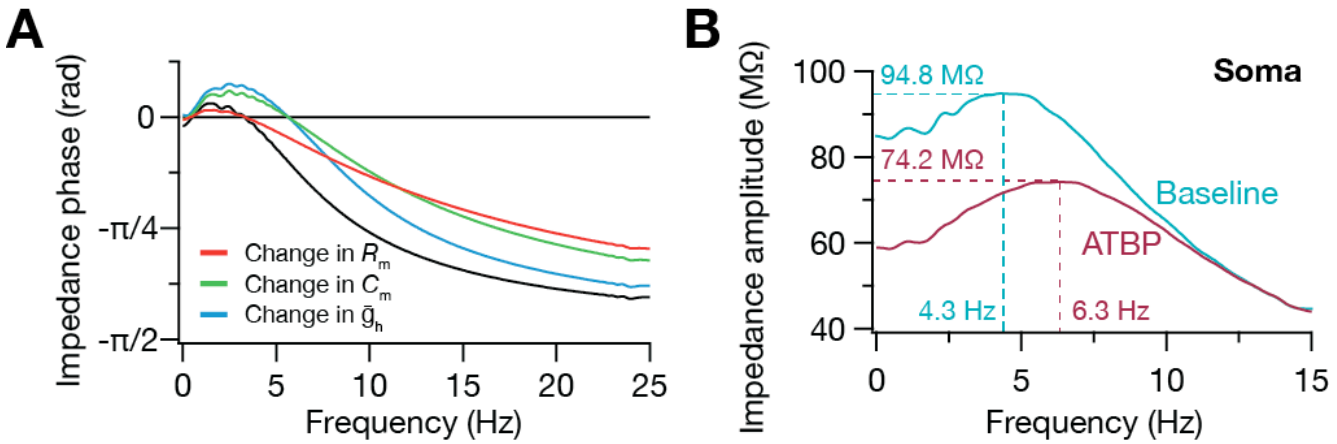

Supplemental Figure 6. ***A****,* Supplemental to Fig. 8*B*. Impedance phase profiles for increasing resonance frequency (f_R) from a baseline (black) only through a two-fold reduction in C_m (green), a three-fold reduction in R_m (red), or a two-fold increase in $\bar{g}_h$ (blue) in the *RCh* circuit (Fig. 8*A*) are shown. ***B****,* Supplemental to Fig. 8*E*. Impedance amplitude profiles of a soma computed during the baseline period and 40 min after ATBP. The increase in resonance frequency (numbers close to the *X*-axis) and the reduction in the maximal impedance amplitude (numbers close to the *Y*-axis) may be noted.